ELEMENTA
Science of the Anthropocene

Delre, A, et al. 2022. Methane and ethane emission quantifications from onshore oil and gas sites in Romania, using a tracer gas dispersion method. *Elem Sci Anth*, 10: 1. DOI: https://doi.org/10.1525/elementa.2021.000111

RESEARCH ARTICLE

Methane and ethane emission quantifications from onshore oil and gas sites in Romania, using a tracer gas dispersion method

Antonio Delre[1], Arjan Hensen[2], Ilona Velzeboer[2], Pim van den Bulk[2], Maklawe Essonanawe Edjabou[1], and Charlotte Scheutz[1,*]

Site-specific methane (CH_4) and ethane (C_2H_6) emission rates from the onshore oil and gas (O&G) sector in Romania were quantified, using the mobile tracer gas dispersion method. As part of the coordinated Romanian Methane Emission from Oil & Gas measurement campaign, this study supported the investigation of CH_4 emissions from the O&G sector around Bucharest. CH_4 emission rates measured at 200 O&G sites were highly skewed with a heavy tail and described by a CH_4 emission factor (EF) with a 95% confidence interval (CI) equal to 0.53 [0.32; 0.79] kg h^{-1} $site^{-1}$. Of the investigated sites, 53% showed CH_4 emission rates below 1 kg h^{-1}, whereas only 6% had emission rates higher than 80 kg h^{-1}, with the highest being equal to 297 kg h^{-1}. CH_4 emission rates from oil wells were not correlated to CH_4 production rates but were negatively correlated to the amount of wastewater produced. C_2H_6 emissions were investigated from 95 O&G sites, the emission rates of which were highly skewed with a heavy tail and described by a C_2H_6 EF with a 95% CI equal to 0.07 [0.04; 0.13] kg h^{-1} $site^{-1}$. Almost 80% of the investigated sites showed C_2H_6 emission rates below 1 kg h^{-1}, and 7% of them had emission rates higher than 9 kg h^{-1}, with the highest being equal to 78 kg h^{-1}. CH_4 emission rates and EFs representing specific types of sites and geographical regions are provided in the manuscript. In terms of magnitude and distribution, these results are in line with published results from measurements at O&G sites in North America, and a natural gas field in the Netherlands. The CH_4 EF calculated in this study is close to the lower range of the majority of values in the literature, whereas C_2H_6 EF is the lowest among the literature values. The study also provided site-specific C_2H_6-to-CH_4 molar ratios in different regions around Bucharest.

Keywords: Site-specific, Romania, EU-27, Gaussian plume model, EU methane strategy, European Green Deal, Climate and Clean Air Coalition

Introduction

Methane (CH_4) emissions into the atmosphere lead to global and local negative impacts on the environment and on human health (Stocker et al., 2013). CH_4 is a potent greenhouse gas with a global warming potential of about 30 times that of carbon dioxide over a 100-year time horizon (Stocker et al., 2013). CH_4 emissions contribute to tropospheric ozone formation, which worsens local air quality and badly affects ecosystem productivity, agricultural yields, and human health (Shindell et al., 2012; Stocker et al., 2013). Due to the relatively short lifetime of CH_4 in the atmosphere (9.1 years, Prather et al., 2012), reducing its emissions would lead to substantial climate benefits in the short term (Shindell et al., 2012). The fossil fuel–based energy sector contributes to about one third of global anthropogenic CH_4 emissions (Kirschke et al., 2013). To tackle global CH_4 emissions, the Oil and Gas Methane Partnership under the United Nations Environment Program Climate and Clean Air Coalition (CCAC) has set a goal of 45% reduction in methane emissions from the oil and gas (O&G) sector over estimated 2015 levels by 2025 and 60%–75% reductions by 2030 (CCAC, 2021). In addition to being part of the CCAC, the European Union (EU) set specific actions in the European Green Deal to decrease CH_4 emissions (European Commission [EC], 2019). In the near future, EU legislation will be revised to adopt accurate CH_4 emission quantifications through direct measurements as EU target standards for reporting purposes via the energy sector (EC, 2020).

Direct atmospheric measurements have shown that national inventories of CH_4 emissions from the O&G sector in North America underestimate the problem (Brandt et al., 2014; Johnson et al., 2017; Zavala-Araiza et al.,

[1] Department of Environmental Engineering, Technical University of Denmark, Kongens Lyngby, Denmark

[2] Department of Environmental Modelling, Sensing & Analysis, TNO, Petten, The Netherlands

* Corresponding author:
Email: chas@env.dtu.dk

2018). CH_4 emissions from a defined geographic region can be quantified by using the bottom-up or the top-down approach (Brandt et al., 2014; Harriss et al., 2015). The bottom-up approach includes methods that measure emissions directly from installations/devices or at site level and scales up these measurements using statistical methods. When using this approach, the collected sample should be representative of the entire investigated population, in order to include the so-called super-emitters that are responsible for the largest share of emissions in the investigated region (Brandt et al., 2014; Rella et al., 2015; Omara et al., 2016). The distributions of CH_4 emission rates measured from O&G regions in North America were highly skewed with a "heavy-tail" of super-emitters, thereby offering a great opportunity to rapidly decrease total CH_4 emissions when these super-emitters are identified (Brandt et al., 2014; Brandt et al., 2016). The most commonly applied measurement methods to quantify CH_4 emissions at site level include ground-based remote-sensing methods relying on measurements of downwind atmospheric gas concentrations and descriptions of the atmospheric dispersion of the target gas (U.S. EPA, 2018). Information about atmospheric gas dispersion can be obtained either by adopting atmospheric models, that is, the Gaussian plume model (GPM; Hensen and Scharff, 2001; Hensen et al., 2006; Fredenslund et al., 2019) and Other Test Method (OTM) 33A (U.S. EPA, 2014), or by releasing a tracer gas (Brantley et al., 2014; Mitchell et al., 2015; Yacovitch et al., 2015; Yacovitch et al., 2017; Robertson et al., 2017; Zavala-Araiza et al., 2018; O'Connell et al., 2019). The top-down approach includes studies that use aircraft, tall towers, ground sampling, and remote-sensing (satellites) to infer CH_4 emissions from a geographic region (Brandt et al., 2014; Schwietzke et al., 2014a; Smith et al., 2015; Johnson et al., 2017).

The extraction, processing, and distribution of fossil fuels are the main anthropogenic sources of ethane (C_2H_6) seeping into the atmosphere (Simpson et al., 2012). Quantifying C_2H_6 emissions from the O&G sector is technically and environmentally important, as the C_2H_6-to-CH_4 molar ratios of a region allow for apportioning sources when CH_4 emissions are investigated via a top-down approach (Schwietzke et al., 2014a; Schwietzke et al., 2014b; Goetz et al., 2015; Smith et al., 2015; Allen, 2016; Mielke-Maday et al., 2019). C_2H_6 not only worsens air quality in several ways by increasing tropospheric ozone formation, but it also enhances the atmospheric lifetime of CH_4 by consuming hydroxide. As a result, it plays a direct and an indirect role as a greenhouse gas through ozone and CH_4, with moderate global impacts (Aikin et al., 1982; Highwood et al., 1999; Collins et al., 2002). Although C_2H_6 emissions from the O&G sector are environmentally important, the literature reports only few studies documenting site-specific C_2H_6 emission rates (Goetz et al., 2015; Yacovitch et al., 2015; Yacovitch et al., 2017) or quantify C_2H_6 emissions at regional scale (Schwietzke et al., 2014a; Smith et al., 2015; Peischl et al., 2018).

In the EU-27, CH_4 emissions from O&G production have been estimated to constitute up to 33% of the total reported European CH_4 emissions caused by the energy sector, making the production of O&G the second most important CH_4 emitter after solid fuel (coal) production (United Nations Framework Convention on Climate Change, 2020). The International Energy Agency estimates that among the EU-27 countries, the Romanian onshore O&G production sector emits 45% of the total recorded for onshore natural gas production and 25% of the total for onshore oil production (IEA, 2020). However, Europe critically lacks CH_4 emission measurement data from onshore O&G sites to help prioritize company actions and government policies for addressing this important emissions source (CCAC, 2021).

The aim of this study was to quantify site-specific CH_4 and C_2H_6 emission rates from the onshore O&G sector in Romania, using a tracer gas dispersion method. The collected dataset was compared with datasets available in the literature. Emission factors (EFs) were computed using the geometric mean with bootstrap simulation. The study was carried out in order to support the regional bottom-up and top-down investigation of CH_4 emissions from the onshore Romanian O&G sector located around Bucharest in the Wallachian plain. The activity was part of the coordinated Romanian Methane Emission from Oil & Gas (ROMEO) measurement campaign, which aimed to investigate CH_4 emissions from O&G production in Romania by using several measurement platforms and deploying numerous emission quantification methods (Röckmann and the ROMEO Team, 2020). The ROMEO measurement campaign included several studies, which will be reported in other scientific papers. In addition to the study hereby described, further quantifications of site-specific CH_4 emissions will be reported in publications investigating the Wallachian plain and other Romanian areas, using quantification methods other than the tracer gas dispersion method. Other publications will assess the bottom-up and top-down approaches gathering the information collected by all teams deploying ground-based methods and aircraft. A publication will investigate the origin of the emissions at the component scale in many O&G sites, by using optical gas imaging devices. A specific paper investigates the CH_4 isotopic signatures of emissions from all investigated areas in Romania (Menoud et al., 2022). The results of the "ROMEO Tracer Team" are described herein.

To the best knowledge of the authors, this is the first time that CH_4 and C_2H_6 emissions have been quantified from the Romanian onshore O&G sector. Only one European study has quantified CH_4 emissions from a natural gas field in the Netherlands (Yacovitch et al., 2018). Additionally, this is the first study that directly reports a large dataset of site-specific C_2H_6 emission rates. The literature offers only 2 studies from which such information can be withdrawn (Yacovitch et al., 2015; Yacovitch et al., 2017), and 1 study reporting emissions from only 3 gas well pads (Goetz et al., 2015). Finally, this study reports gas emission quantifications performed at individual production gas and oil wellheads instead of commonly measured groups of wellheads.

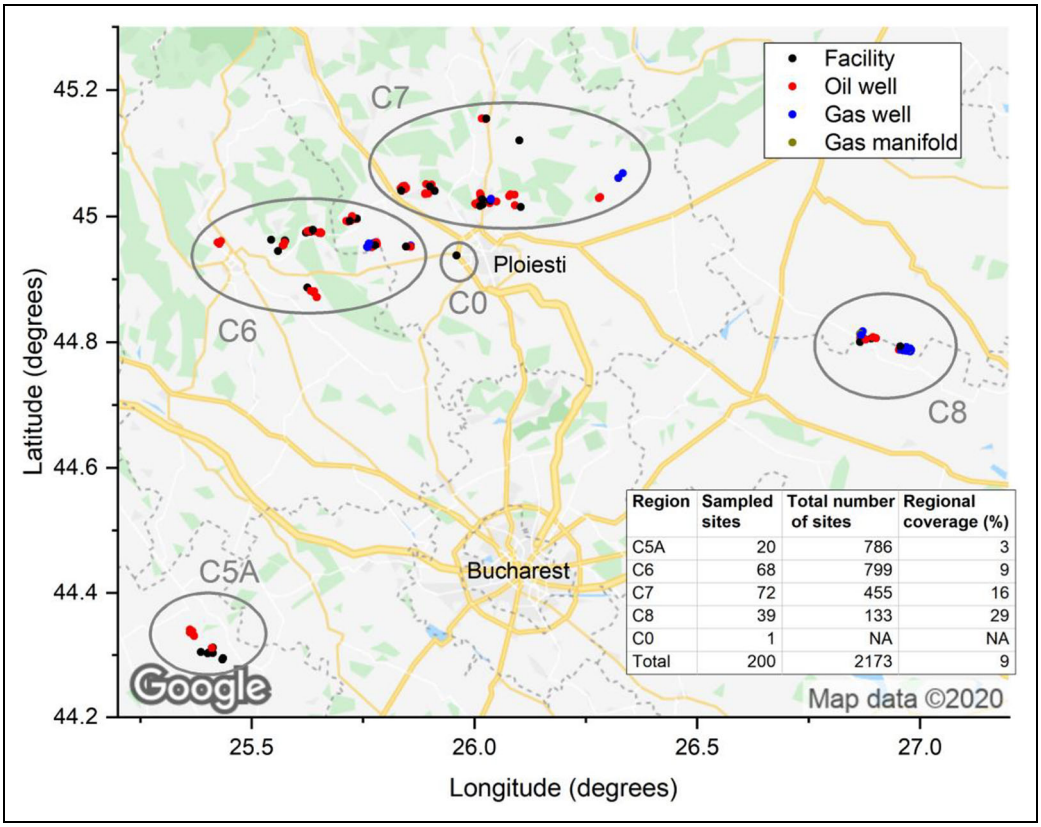

Region	Sampled sites	Total number of sites	Regional coverage (%)
C5A	20	786	3
C6	68	799	9
C7	72	455	16
C8	39	133	29
C0	1	NA	NA
Total	200	2173	9

Figure 1. Location of the sampled sites grouped by region, as defined in the Romanian Methane Emission from Oil & Gas coordinated campaign. Sites in the area were grouped into 5 regions as shown on the map (Google ©). NA = not available. DOI: https://doi.org/10.1525/elementa.2021.000111.f1

Material and methods

Description of the investigated area

The sampled O&G sites were located in 5 Romanian counties around Bucharest (Prahova, Buzau, Ialomita, Dambovita, and Teleorman). **Figure 1** shows the location and type of site grouped in regions as defined by the ROMEO campaign coordinators. Each region was divided into 4–9 clusters, each containing between 10 and 583 sites (O&G production wells and facilities). Criteria used to group the sites within regions and clusters are described along with the sampling strategy. Individual O&G production wellheads were considered point sources, while facilities like oil parks, production batteries, gas compressors, and so on, were considered area sources, as they can have multiple gas leakages and outlets.

From the geological perspective, all investigated regions are located in the Carpathian-Balkanian Basin Province as defined by Pawlewicz (2007). Regions C0, C6, and C7 (**Figure 1**) lie in the assessment unit of the Romanian Ploiesti Zone, which is part of the Dysodile Schist–Tertiary total petroleum system. In particular, C0, C6, and C7 lie in the subunit called Diapir Folds zone, which follows the Carpathian bend and it is featured by the Sub-Carpathian nappe (Pawlewicz, 2007). The Diapir Folds zone is characterized by source rocks as Oligocene dysodile schist and possibly middle Miocene and Pliocene black shale (Dinu et al., 1996). Hydrocarbons in the Sub-Carpathian nappe are accumulated in Oligocene and in lower and upper Miocene sandstones. In particular, the reservoirs of the Diapir Folds zone are mainly sandstones with high porosity and permeability (Dinu et al., 1996). Regions C5A and C8 (**Figure 1**) lie in the assessment unit of the Moesian Platform, which is part of the Moesian Platform Composite total petroleum system. The Moesian platform is limited to the north by the foredeep of the Carpathian Mountains, it extends under the Danubian lowlands of Romania and occupies the northern part of Bulgaria (Pawlewicz, 2007). Source rocks of this platform include both clastic and carbonate rocks. Although the main reservoirs of the Moesian platform are upper Miocene clastic rocks, lower Cretaceous carbonate reservoirs are also present. The Rumanian part of the Moesian platform has reservoirs distributed throughout the stratigraphic column and it has many different lithologies (Pawlewicz, 2007). O&G are mainly in Mesozoic rocks, and they are equally distributed between the Permian-Triassic, Middle Jurassic (Dogger), and Cretaceous (Tari et al., 1997).

Measurement method

CH_4 and C_2H_6 emission quantifications from the O&G sites were obtained by deploying the mobile tracer gas dispersion method (MTDM)—a ground-based remote-sensing technique previously used to quantify air emissions from the O&G sector (Lamb et al., 1995; Shorter et al., 1997; Allen et al., 2013; Goetz et al., 2015; Mitchell et al., 2015; Omara et al., 2016; Yacovitch et al., 2017; Roscioli et al., 2018; Zavala-Araiza et al., 2018). MTDM combines the controlled, constant release of a tracer gas from

the emitting site with the detection of downwind atmospheric concentrations of the tracer and the target gas. Furthermore, it is based on the principle that long-lived atmospheric gases disperse in the same way in the atmosphere, and therefore, even when the plume dilutes, the concentration ratio remains constant over space and time. As a consequence, the emission rate of the target gas is calculated by using downwind concentration enhancements of the target gas and the tracer gas, as reported in Equation 1:

$$E_{tg} = Q_{tr} \cdot \frac{\int_{\text{plume start}}^{\text{plume end}} (C_{tg} - C_{tg\ \text{baseline}})\mathrm{d}x}{\int_{\text{plume start}}^{\text{plume end}} (C_{tr} - C_{tr\ \text{baseline}})\mathrm{d}x} \cdot \frac{MW_{tg}}{MW_{tr}}, \quad (1)$$

where E_{tg} is the target gas emission rate in units of mass per time, Q_{tr} is the known tracer release rate in units of mass per time, C_{tg} and C_{tr} are the detected plume mole fractions within the plume traverse in parts per billion (ppb), $C_{tg\ \text{baseline}}$ and $C_{tr\ \text{baseline}}$ are baseline mole fractions of the target and the tracer gas (ppb) and MW_{tg} and MW_{tr} are the molecular weights of the target gas and tracer gas, respectively (Scheutz et al., 2011). Equation 1 is valid only if the combination between the release of the tracer gas and the distance of the plume traverse allow an adequate simulation of the target gas emissions by means of the tracer gas release (Delre et al., 2018). Acetylene (C_2H_2) and nitrous oxide (N_2O) were used as tracer gases due to their long atmospheric lifetime, constant atmospheric background, possibility to be detected with analytical instruments having enough precision and detection frequency, relatively low costs, and the fact that they are not emitted from O&G sites (Delre, 2018). The release of C_2H_2 has the advantage of producing low environmental impacts. Conversely, N_2O is a potent greenhouse gas (Stocker et al., 2013), but its use is considered a fair compromise due to the importance of the obtained information. Both C_2H_2 and N_2O are largely used as tracers in O&G investigation (Allen et al., 2013; Goetz et al., 2015; Omara et al., 2016; Yacovitch et al., 2017; Roscioli et al., 2018; Zavala-Araiza et al., 2018).

Measurements were carried out with 2 vehicles equipped with laser gas analyzers. Atmospheric air was sampled from the roof of the vehicles and conveyed to the gas analyzers, which detected mole fractions of the target and tracer gases. One vehicle sampled air from approximately 2 m above the ground. A first small external pump (GAST 8R1110-201-1049), with a flow equal to 3.4 L min^{-1}, pulled the air until a split to the atmosphere located just before the analyzers, which were equipped with a serial pump working with a flow equal to about 0.4 L min^{-1}. The polypropylene sample lines were about 1.9 m long with internal and external diameters of 4 and 5 mm, respectively. Swagelok fittings avoided any contamination of the samples. This vehicle was equipped with 2 gas analyzers based on cavity ring-down spectroscopy, one of which detected CH_4 once per second (G2401, Picarro, Inc., Santa Clara, CA), with a precision of 1.7 ppb and a response time of 2s, while the other detected N_2O and C_2H_2 every 3s (S/N JADS2001, Picarro, Inc., Santa Clara, CA), with a precision of 21.1 and 1.6 ppb, respectively, and a response time of about 7s. Gas analyzer precision is reported here as 3 times the standard deviation of 6 min constant concentration reading. Each gas analyses used 2 internal filters for particulate matter, which are specific for Picarro analyzers. The gas analyzers G2401, detecting CH_4, and S/N JADS2001, detecting C_2H_2 and N_2O, were calibrated with 3 calibration gases certified by the World Meteorological Organization (WMO). Three mole fractions within the detection interval of the instrument were used to produce a calibration line, which was used to adjust the mole fractions recorded in the field. Calibration gases had the following concentrations for specific gases: 5, 25, and 51 ppm for CH_4; 5, 15, and 40 ppb for C_2H_2; 0.4, 69.6, and 149.8 ppm for N_2O.

The other vehicle sampled air from approximately 3 m above the ground. A pump (Agilent IDP-15 Dry Scroll Pump), with a flow equal to 5 L min^{-1}, pulled the air through the polypropylene sample line 1 m long with internal and external diameters of 5 and 6 mm, respectively. Swagelok fittings avoided any contamination of the samples. This vehicle was equipped with a dual laser trace gas monitor based on Tunable Infrared Laser Direct Absorption Spectroscopy, using a quantum cascade laser and an interband cascade laser to measure CH_4, C_2H_6, N_2O, CO_2, and CO simultaneously (Aerodyne Research Inc., Billerica, MA) at 1 Hz with a precision of 2.4, 0.1, 0.1, 386.3, and 2.5 ppb, respectively. This gas analyzer had a response time equal to about 2s and was calibrated using calibration gases certified by the WMO, as used in the Integrated Carbon Observation System at the Cabauw tall tower in the Netherlands. The calibration operations were performed multiple times during a measurement day to assure accurate detection of target gases. Calibration gases had the following mole fractions for specific gases: 1,975 and 4,695 ppb for CH_4; 332.6 and 331.9 ppb for N_2O; 412.5 and 427.4 ppm for CO_2; 185.1 and 165.8 ppb for CO.

Tracer gases were released from gas cylinders at constant flow rates, using calibrated flow meters, pressure reducers and critical orifices, and the total amount of released tracer gas was quantified by weighing the cylinder before and after release.

When investigating a specific site, measurements consisted of a screening phase and a quantification phase. During the screening phase, the gas analyzer was driven around the target site to record atmospheric concentrations of the target gas. A site was defined as an emitter when concentrations of the downwind target gas showed an enhancement compared to concentrations detected upwind from the site. When beginning measurements at each site, atmospheric concentrations were measured upwind and downwind of the site, to check for potentially disturbing off-site sources, which were mostly other O&G sites and farms. The plume of the target gas, generated by the disturbing off-site sources, would have overlapped with the plume of the target site, resulting in a distortion of the real emission rate. An investigated site was considered to be affected by a disturbing off-site source, if the

upwind screening showed a plume of the target gas with a concentration peak higher than 3 times the size of the background noise recorded in absence of emitting sources. The same threshold was already adopted to distinguish the presence of a signal in sequential records (Shrivastava and Gupta, 2011). If a disturbing off-site emitter was found close to the target site, measurements were carried out under different wind conditions, when the plume from the target site could be distinguished from the plume coming from the off-site source.

In the quantification phase, a constant flow from the tracer gas cylinder was released via flexible tubing placed as closely as possible to the emission location. At O&G wells, which were always protected by a fence, the flexible tube was pushed to the location of the well borehole by using a rod. At large area sources (e.g., sites containing oil tanks and high-pressure injection systems), the tracer could not be released from inside the site, due to a lack of access. In this case, the tracer was released near the fence of the target area, so that the distance of the target and the tracer gas release to the street where measurements were subsequently conducted was similar. This assured that both gases underwent (as much as possible) similar conditions regarding mixing and transport, which also included similarly sized vegetation or objects between the source and the measurement transect.

During the quantification phase, several plume traverses (on average 9 traverses) were performed downwind at a suitable distance away from the target site. In each plume traverse, the plume was completely crossed, and the background concentrations of target and tracer gas were identified on both sides of the plume, to establish a baseline that would be subtracted from the enhanced concentrations (Equation 1), thereby obtaining only the target source's contribution to atmospheric concentrations. Depending on the physical size and layout of the site, site accessibility, in terms of roads, drivable fields and measurement distance, varied from 20 to 620 m. The driving speed was about 15–25 km h^{-1}. Quantification time at a single site varied between about 30 and 60 min.

The emission rate of a site's target gas was given as the average value of emission rates calculated based on multiple plume traverses. The variability in the quantification of an individual site was given at a 95% confidence interval (CI) of emission rates calculated based on multiple plume traverses, which were assumed normally distributed. The 95% CI was calculated by multiplying for each site the standard error of the mean by 1.96, which is the 97.5 percentile point value of the standard normal distribution. The variability in the quantification of an individual site was reported as a percentage of the average value, while total uncertainty was calculated as the square root of the sum of the squares of the method's uncertainty and the variability in the quantification. More information about the uncertainty budget is provided in Section S1.

During the screening phase, some sites showed the same atmospheric concentrations of the target gas upwind and downwind, and target gas emission rates were defined as being below detection limit (BDL). This means that the concentrations recorded downwind of the investigated site did not show any plume peak higher than 3 times the size of the background noise recorded upwind (Shrivastava and Gupta, 2011). The MTDM detection limit was calculated according to Delre et al. (2017), using the GPM described in Equation 2:

$$C(x,y,z) = \frac{Q}{2\pi u \sigma_y(x)\sigma_z(x)} \cdot \left(e^{-0.5\left(\frac{z-H}{\sigma_z(x)}\right)^2} + e^{-0.5\left(\frac{z+H}{\sigma_z(x)}\right)^2} \right) e^{-0.5\left(\frac{y}{\sigma_y(x)}\right)^2} \quad (2a)$$

$$\mathrm{BDL} = Q_{\min} = \frac{C_{\min}(x,0,z)2\pi u \sigma_y(x)\sigma_z(x)}{\left(e^{-0.5\left(\frac{z-H}{\sigma_z(x)}\right)^2} + e^{-0.5\left(\frac{z+H}{\sigma_z(x)}\right)^2} \right) e^{-0.5\left(\frac{y}{\sigma_y(x)}\right)^2}}, \quad (2b)$$

where in Equation 2a, C is the concentration (kg m^{-3}) in any given downwind plume point (x, y, z) measured from the source, Q is the emission rate (kg s^{-1}), u is wind speed (m s^{-1}), $\sigma_y(x)$ and $\sigma_z(x)$ are the dispersion coefficients (m), and is emission height above ground level (m).

Equation 2b was obtained directly from Equation 2a to calculate the MTDM detection limit (BDL), that is, the lowest measurable emission rate $Q_{\min}$. Three features influence $Q_{\min}$: the precision of the analytical instrument, the measurement distance, and weather conditions. The smallest measurable downwind peak plume concentration $C_{\min}(x, 0, z)$ was set at 3 times the size of the background noise of the target gas determined for the specific measurement period (Shrivastava and Gupta, 2011). $C_{\min}(x, 0, z)$ is the concentration at x m away from the source, in the middle of the plume traverse ($y = 0$) and at the roof of the measurement platform (z m from the ground), where atmospheric concentrations were sampled. Horizontal and vertical dispersion coefficients, namely $\sigma_y(x)$ and $\sigma_z(x)$, were applied by following Briggs (1974), and atmospheric stability classes were obtained according to Pasquill (1974), using a weather station recording temperature, wind speed, wind direction, atmospheric pressure (Kestrel 5500 Weather Meter) placed close to the emitting site. By definition, the MTDM detection limit is site- and time-specific when using the same analytical platform (Delre et al., 2017).

At some sites, the MTDM could not be applied due to technical maintenance required for the gas analyzer detecting the tracer gas. In these cases, the GPM was applied. The procedure for the site investigation was as described for the MTDM, with the exception of the tracer release process and calculation of the emission rate of the target gas. In this case, the emission rate of the target gas Q was obtained from Equation 2a. The downwind target gas concentration $C(x, y, z)$ was the fitted peak concentration of a single plume traverse, and concentrations recorded crossing the plume were fitted with a Gaussian function in OriginPro 2019 ® (OriginLab, 2019). Choosing the fitted peak value to the actual peak recorded during the plume traverse allowed for weighting the entire plume traverse rather than considering only one detection point. Additionally, using the fitted peak value allowed for more accurate measurements than using the detected peak value (Section S2). Similar to the assessment of the MTDM detection limit, dispersion coefficients were

chosen following Briggs (1974), whereas atmospheric stability classes were obtained according to Pasquill (1974), using a weather station placed close to the emitting site. Quantification variability was reported in the same way as for the MTDM (Section S1).

At 3 sites, plume traverses could not be performed downwind of the emitting source. Therefore, a static tracer gas dispersion method (STDM) was applied. When applying the STDM, stationary tracer and target gas measurements are performed downwind of the target site. In this case, the emission rate was still calculated by using Equation 1, but the target and tracer gas concentration ratio recorded over several minutes was used instead of the ratio of the integrated plume traverse concentrations (Samuelsson et al., 2018).

During the ROMEO campaign, some emitting sites' emissions could not be properly quantified by using any of the methods reported above, due to wind conditions and the unsuited layout of the sites and their surroundings. In these cases, the emission rate was calculated by applying the GPM, using the peak concentration of the target gas recorded a few meters downwind of the site. This method considered only one concentration record and therefore was simply named "Estimate."

Three types of evaluations were thus used for investigating the O&G sites: quantification (via MTDM, GPM, and STDM), estimation, and the assessment whether the emission rate was BDL. The adopted quantification and estimate methods had different uncertainties that were assessed by following Fredenslund et al. (2019; see Section S1). Method uncertainty and quantification variability, or estimation, are 2 factors that define the total uncertainty of quantified, or estimated, emission rates, expressed as percentages of the emission rate and calculated with a 95% CI (see Section S1).

At 41 sites, all methods were applied. A statistical model provided the mathematical relationships between MTDM and GPM, and between MTDM and the estimate. These relationships were used to correct results obtained using GPM and the estimate, which usually underestimated emissions quantified using MTDM. More details about the correction procedure are provided in Section S3.

Determination of the C_2H_6-to-CH_4 molar ratio

The C_2H_6-to-CH_4 molar ratio for each site was determined by taking the ratio between the integrated plume concentrations of ethane and methane as reported in Equation 3:

$$C_2H_6 - \text{to} - CH_4 \text{molar ratio} = 100 \cdot \frac{\int_{\text{plume start}}^{\text{plume end}} (C_{C_2H_6} - C_{C_2H_6\ \text{baseline}})\mathrm{dx}}{\int_{\text{plume start}}^{\text{plume end}} (C_{CH_4} - C_{CH_4\ \text{baseline}})\mathrm{dx}}, \quad (3)$$

where $C_{C_2H_6}$ and C_{CH_4} are the detected plume mole fractions of ethane and methane within the plume traverse in ppb and $C_{C_2H_6\ \text{baseline}}$ and $C_{CH_4\ \text{baseline}}$ are baseline mole fractions of ethane and methane (ppb).

Determination of EFs

EFs and corresponding 95% CIs were calculated by using a non-parametric bootstrap simulation implemented in the R package *tidyboot* (Mika and Daniel, 2021). The calculation of the EF did not include the uncertainty of each observation in the datasets due to model limitations. Nevertheless, this was overcome by the high numbers of non-parametric bootstrap samples (10,000), which also helped compute the CI without assuming a specific distribution of the data (Chernick and LaBudde, 2011). CH_4 and C_2H_6 EFs were determined for the complete dataset as well as for selected sub-datasets such as different types of sites (e.g., gas wells, oil wells, and facilities) and different regions in the investigated area. The nonparametric approach was applied because neither the complete dataset nor studied sub-datasets passed the statistical test for lognormal distribution and exponential distribution (Table S3). The datasets were tested for these 2 types of distributions, as emission data previously reported in the literature had shown to be lognormal or exponentially distributed. Brantley et al. (2014), Rella et al. (2015), Yacovitch et al. (2017), and Zavala-Araiza et al. (2018) reported that CH_4 emission rates followed a lognormal distribution, whereas Yacovitch et al. (2015) reported CH_4 emission rates to follow an exponential distribution. In this study, the geometric mean was chosen as central value of the emission distribution and thus corresponded to the final EF because it is considered to better describe very skewed datasets (Reimann et al., 2008; Millard, 2013). Currently, there is no consensus in the literature on which central value should be used as EF when using nonparametric bootstrapping and both geometric mean, arithmetic mean and median have been used (Brantley et al., 2014; Rella et al., 2015; Brandt et al., 2016; Robertson et al., 2017; Riddick et al., 2019). An overview of methods and central values used to compute EFs reported in the literature is provided in Table S9.

The collected CH_4 and C_2H_6 emission datasets were compared with datasets available in the literature. No distinction was made between different types of sites because most of the studies reported in the literature do not specify the type of the emitting source (gas well vs. oil well, single wellheads vs. groups of wellheads, etc.) of each reported emission rate (cf. Table S6). For a consistent comparison, EFs for literature datasets were calculated following the statistical inferring method adopted in this study (nonparametric bootstrapping with geometric mean as central value). This assured that the results of the comparison were not affected by the approach chosen for the calculation of the EFs in the different studies. It is hereby emphasized that this was done solely to ensure an optimal basis for comparison and not because the authors do not recognize other methods of calculating EFs or original EFs provided in referenced studies. For completeness and potentially future comparisons, full statistic descriptions of this study's datasets as well at the analyzed datasets from literature are provided in the paper including arithmetic mean, median, minimum, maximum, variance, skew, and kurtosis.

Sampling strategy

In the ROMEO campaign, the coordinators divided the territory to be investigated into regions and site clusters. Regions included parts of the territory where sites had similar features regarding location density (high and low density) and magnitude of O&G production (high and low production). Within regions, clusters of sites were defined in order to facilitate administrative applications for flight permissions. The campaign coordinators assigned to the "ROMEO Tracer Team" the specific regions and clusters to be investigated. Measurements reported in this study were performed from November 1 to 18, 2019.

The sampling strategy for the measurement platforms described in this study consisted of 2 main phases: a desktop analysis and an in-field action. During the desktop analysis, the investigated clusters were split among measurement teams working in the same region, so that a single measurement platform was in charge of investigating sites located in specific clusters. Subsequently, the locations of individual sites were analyzed and potential quantifiable sites were identified according to the wind direction and road access. During in-field actions, the potential quantifiable sites were targeted first by performing screening and quantification as previously described. Thereafter, the remaining sites in the clusters assigned to the measuring platform were screened, independently of the suitability of the wind direction of that day. If elevated methane concentrations were recorded during the screening but quantification could not be done on the specific day, this was noted and the site was revisited when the wind blew in a wind direction favorable for quantification. Some sites were not accessible for screening and quantification due to rough terrain, time constraints, interfering sources, or other local restrictions, and thus in some clusters it was not possible to investigate every site, which may cause spatial bias to the sampled sites. The collected sample was not biased by the emission magnitude of the site, as sites that were screened and did not exhibit any target gas concentration enhancement were defined as "BDL," while the others were either quantified or estimated. In total, 200 sites were sampled, including O&G wells, gas manifolds, and various area sources such as facilities containing oil parks, production batteries, compressors, and so on.

Results and discussion

Dataset description

Table 1 provides an overview of the investigated sites in terms of type of site (facility, oil well, gas well, or gas manifold) and type of evaluation (quantification, estimate, or BDL). In total, CH_4 emissions were investigated at 200 O&G sites, which were mainly oil wells (61%), facilities (21%), and gas wells (17%). Oil wells had an average age of 27 years and produced on average 68 Mg of oil year^{-1} per well. Gas wells had an average age of 39 years and produced on average about 215,400 SCM of natural gas year^{-1} per well. CH_4 emission rates were quantified at most of the investigated sites (38%) and estimated at 34% of the sites, and 28% showed emission rates BDL (**Table 1**). Of the CH_4 emission quantifications, 70% were performed using the tracer information. Among the 200 investigated sites, there were 20 nonproducing sites according to the operator (16 oil wells and 4 gas wells). A nonproducing site is defined as an oil or gas well where, at the time of measurement, there was no production due to low reservoir pressure, technical issues, and so on. At some sites, oil or gas flow was temporarily stopped by shutting down valves, capping the well or blocking the flow. C_2H_6 emissions were assessed at 95 of the 200 sites, because only one of the 2 measuring platforms was able to measure this gas. It was mainly investigated at oil wells (66%) and facilities (32%). C_2H_6 emission rates were quantified at 11% of the investigated sites and estimated at 49% of the sites, and 17% showed emission rates BDL (**Table 1**). C_2H_6-to-CH_4 molar ratios were measured at 76 sites: 28 facilities (37% of the sites), 1 gas well (1% of the sites), and 47 oil wells (62% of the sites). Locations of the investigated sites are reported in **Table 1** are shown in Figure S2.

Table 1. Overview of the investigated sites. DOI: https://doi.org/10.1525/elementa.2021.000111.t1

Investigated Gas	Total Sites	Site Description (# Sites; % of Total Investigated Sites)	Type of Evaluation (# Sites; % of Total Investigated Sites)		
			Q	*E*	BDL
CH_4	200	Facilities (42; 21%)	24; 12%	13; 6%	5; 3%
		Gas manifolds (3; 2%)	3; 2%	0; 0%	0; 0%
		Gas wells (33; 17%)	6; 3%	11; 5%	16; 8%
		Oil wells (122; 61%)	42; 21%	46; 23%	34; 17%
C_2H_6	95	Facilities (30; 32%)	19; 20%	9; 9%	2; 2%
		Gas wells (2; 2%)	0; 0%	1; 1%	1; 1%
		Oil wells (63; 66%)	10; 11%	37; 39%	16; 17%

Detection limit is calculated according to Delre et al. (2017). # sites = number of investigated sites; *Q* = quantification; *E* = estimate (screened sites showing target gas concentrations above background levels); BDL = below detection limit (screened sites showing target gas concentrations at background levels).

Table 2. Descriptive statistics of CH_4 emission rates grouped by type of site (facility, gas wells, and oil wells) and region.
DOI: https://doi.org/10.1525/elementa.2021.000111.t2

Grouping	Number of Observations	Geometric Mean (kg h^{-1})	Arithmetic Mean (kg h^{-1})	Median (kg h^{-1})	Min. (kg h^{-1})	Max. (kg h^{-1})	Variance	Skew	Kurtosis
Complete dataset	200	0.51	13	0.79	$3{\cdot}10^{-4}$	297	1,127	4.8	30
Facilities in all regions	42	2.0	21	6.2	$3{\cdot}10^{-4}$	297	2,679	4.0	17
Gas wells in all regions	33	0.24	19	0.10	$8{\cdot}10^{-4}$	198	1,985	2.5	6.0
Oil wells in all regions	122	0.36	7.9	0.53	$7{\cdot}10^{-4}$	99	361	3.2	10
All sites in region C5A	20	0.62	9.1	0.82	$7{\cdot}10^{-4}$	99	495	3.3	11
All sites in region C6	68	0.91	15	1.6	$9{\cdot}10^{-4}$	198	1,252	3.2	11
All sites in region C7	72	0.58	13	0.71	$8{\cdot}10^{-4}$	297	1,494	5.8	38
All sites in region C8	39	0.12	9.3	0.08	$3{\cdot}10^{-4}$	107	624	2.8	7.0
Gas wells in all regions without nonproducing	29	0.28	22	0.15	$1{\cdot}10^{-3}$	198	2,210	2.3	4.7
Oil wells in all regions without nonproducing	106	0.52	9.1	0.81	$1{\cdot}10^{-3}$	99	405	3.0	8.3

One observation in region C0 and 3 observations at gas manifolds were not included in the type of site and region subsets.

The geometric mean is the exponential transformation applied to the mean of the log-transformed data and expressed as follows: $\hat{y} = \sqrt[n]{\prod y}$.

Arithmetic mean is the sum of the observations divided by the number of observations, and expressed as follow: $\bar{x} = \frac{1}{n}\sum_{i=1}^{n} x_i$.

Kurtosis is a measure indicating whether the data distribution is flat or peaked (Reimann et al., 2008; kurtosis equal to 0 indicates a normal distribution, whereas kurtosis [in absolute value] higher than ± 2 is considered extreme).

CH_4 emission rates and factors

CH_4 emission rates ranged from $3.0{\cdot}10^{-4}$ to 297 kg h^{-1}, and they were positively skewed with a heavy tail (**Table 2**). More than half of the sites, namely 105 out of 200, had a CH_4 emission rate below 1 kg h^{-1}, whereas only 11 sites had emission rates higher than 80 kg h^{-1}. A small portion of investigated sites (5%) contributed to about 52% of the total measured CH_4 emission rate (complete dataset in **Figure 2A1**) and had an emission rate higher than 84 kg h^{-1} (complete dataset in **Figure 2A2**). Similar results were obtained when the dataset was grouped into the type of site (facilities, gas wells and oil wells) and investigated regions (**Table 2** and **Figure 2A1** and **A2**). **Figure 2B** illustrates the CH_4 emission rates from all 200 sites, grouped by the type of evaluation. At all sites where CH_4 emission rates were quantified or estimated, the detection limit was always smaller (in most cases 1–2 orders of magnitude smaller) than the measured emission values (Figure S3).

The CH_4 EF with 95% CI for the complete dataset (including sites with emissions below detection) was equal to 0.53 [0.32; 0.79] kg h^{-1} $site^{-1}$ (**Figure 2C**). Among the investigated types of sites, facilities were the largest emitters with a CH_4 EF equal to 2.3 [0.66; 5.3] kg h^{-1} $site^{-1}$. The CH_4 EF of facilities had the largest 95% CI, due to the largest range of CH_4 emission rates. Oil wells and gas wells had similar CH_4 EFs equal to about 0.35 kg h^{-1} $site^{-1}$. Among the investigated regions, C8 reported the lowest CH_4 EF with 95% CI, equal to 0.14 [0.04; 0.39] kg h^{-1} $site^{-1}$, whereas the other regions had a CH_4 EF equal to about 0.81 kg h^{-1} $site^{-1}$. CH_4 EF values are reported in Table S4 and shown in **Figure 2C**.

CH_4 emission rates were found to be negatively correlated to the produced wastewater at oil wells ($r_s = -0.52$). No other correlations were found with other production factors or site age. More information regarding the correlation test is available in Section S5.2.

Comparison with CH_4 emissions reported in the literature

The collected CH_4 emission rate dataset was compared with studies investigating onshore O&G activities. Table S6 provides an overview of these studies, which were grouped according to those including sites with emissions below the detection limit of the adopted measurement method, and those that disregarded them. To facilitate the comparison, the current study was represented by the complete dataset and the dataset without sites with emissions below detection. The complete dataset for the current study is the second largest dataset available in the literature after Caulton et al. (2018), which counts 667 investigated sites. The literature reports mostly studies carried out in Canada and the United States, with only one exception (Yacovitch et al., 2018) reporting CH_4 emissions from 16 sites in a Dutch natural gas field. The majority of the datasets were very positively skewed with

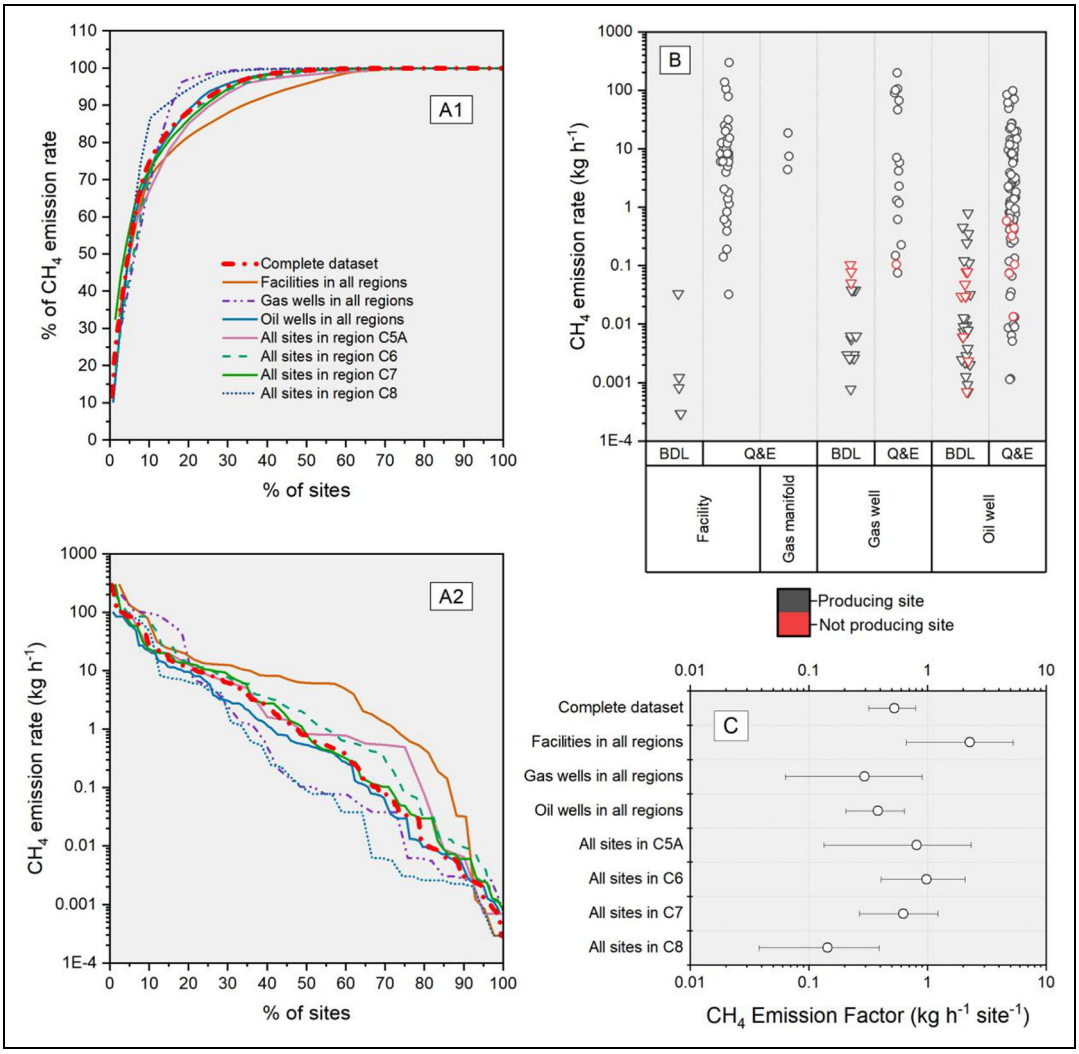

Figure 2. Overview of CH_4 emissions. (A1) Skew in the CH_4 emission rates grouped by region, type of site, and complete dataset. CH_4 emission rates are ranked in descending order. (A2) Measured CH_4 emission rates ranked in descending order versus cumulative percentage of sites. CH_4 emission rates are grouped by region, type of site, and complete dataset. (B) CH_4 emission rates grouped by type of site and type of evaluation: below detection limit (BDL), quantification and estimate (Q&E). (C) CH_4 emission factors (EF) with a 95% confidence interval for several subsets in the current study. CH_4 EFs values are reported in Table S4. DOI: https://doi.org/10.1525/elementa.2021.000111.f2

a heavy tail, and there were very few exceptions (Table S7 and Figure S5). For a more direct comparison, skew and CH_4 emission rate contributions in the datasets are visualized in Figure S6.

Figure 3 compares EFs calculated based on CH_4 emission datasets from onshore O&G activities reported in the literature (Table S8 for more details). Literature CH_4 EFs range between 0.18 and 14 kg h^{-1} $site^{-1}$ in studies including sites with emissions below detection, and between 0.6 and 1,360 kg h^{-1} $site^{-1}$ in studies excluding sites with emissions below detection (**Figure 3**). The complete dataset for the current study had a CH_4 EF with a 95% CI equal to 0.53 [0.32; 0.79] kg h^{-1} $site^{-1}$, whereas the dataset excluding sites with emissions below detection of the current study had a CH_4 EF with a 95% CI equal to 2.3 [1.5; 3.5] kg h^{-1} $site^{-1}$. These 2 CH_4 EFs are close to the lower and upper ranges (0.5 and 3.0 kg h^{-1} $site^{-1}$), respectively, of the majority of CH_4 EFs calculated based on literature datasets (**Figure 3** and Table S8). The inclusion in the current dataset of 55 observations with emissions BDL is a key factor in obtaining a representative EF that can be used for upscaling emissions to a larger area (the bottom-up approach). The analysis of CH_4 EFs from the literature showed that studies reporting CH_4 emission rates from the same basins provide different CH_4 EFs (e.g., Robertson et al., 2017, and Yacovitch et al., 2017, reporting from the Denver-Julesburg [DJ] basin, and Fayetteville [FV] gas play; **Figure 3**).

The scientific literature also reports studies where the datasets were not made available, and EFs for direct comparison could thus not be calculated using the method adopted in this study. The first investigations into CH_4 emission rates from onshore O&G sites were performed in the United States in the 1990s (Lamb et al., 1995; Shorter et al., 1997), reporting emission rates from production sites (0.43–1.7 kg h^{-1}) that were within the intervals found in the current study. However, emissions from

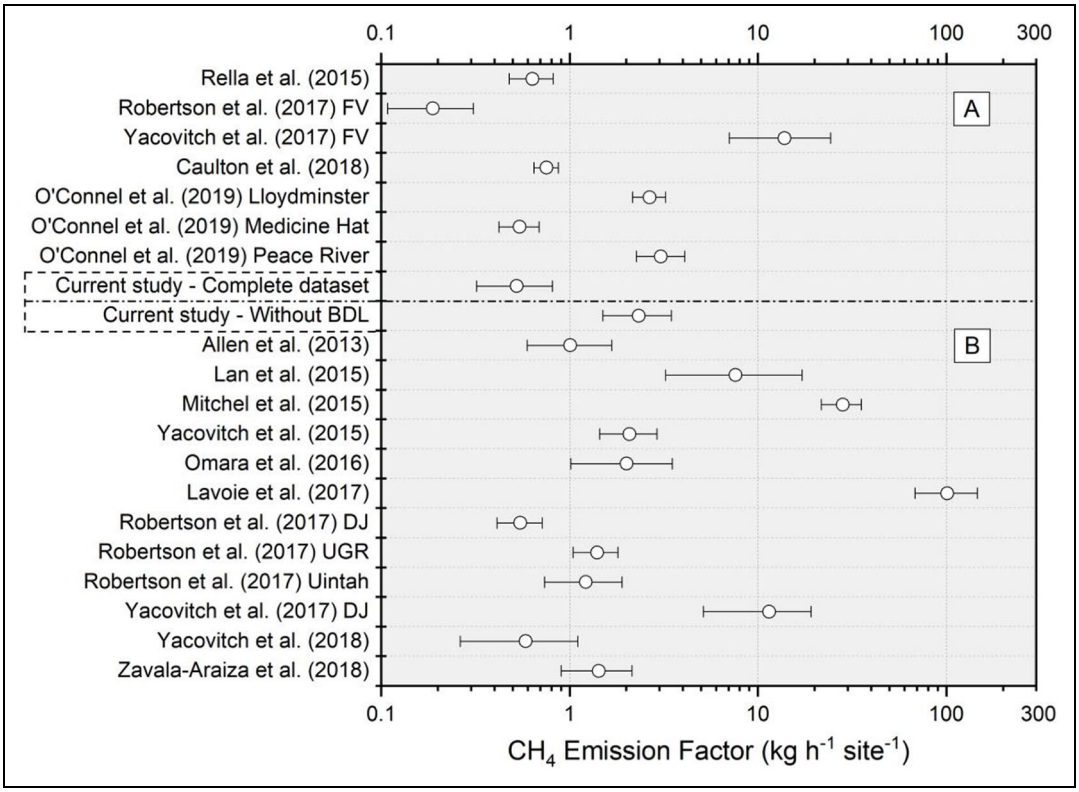

Figure 3. CH_4 emission factors based on available literature datasets. (A) Studies including measurements below detection limit (BDL). (B) Studies not including measurements BDL. Data for CH_4 EF are available in Table S8. DOI: https://doi.org/10.1525/elementa.2021.000111.f3

facilities (0.43–878 kg h^{-1}) were generally higher than those reported by the current study (**Figure 2C**). Nevertheless, Lamb et al. (1995) and Shorter et al. (1997) provide emission rates smaller than Lan et al. (2015), with CH_4 emission rates up to 2,119 kg h^{-1} (Table S7). Goetz et al. (2015) investigated 12 Pennsylvanian sites, using the MTDM, while Brantley et al. (2014) investigated 224 sites in Texas, Colorado, and Wyoming, by using the OTM 33A and including investigated sites defined as BDL. Combined, these 2 studies report CH_4 emission rates from O&G sites in the United States, providing emission rates within the range provided by the current study (0.83–14 kg h^{-1} for well pads, 17–205 kg h^{-1} for compression stations; Brantley et al., 2014; Goetz et al., 2015).

CH_4 emission variability

A comparison between the CH_4 emission rate variability of individual quantifications and the uncertainty of the MTDM method showed that CH_4 emissions varied significantly during the time intervals (30–60 min) when the plume traverses were performed. **Figure 4** compiles the variability of quantifications reported by the current study and 3 other studies reported in the literature applying the MTDM at O&G sites. Additionally, **Figure 4** illustrates a conservative estimate of the emission quantification uncertainty, using MTDM reported by Fredenslund et al. (2019) and based on large-scale controlled release tests (i.e., the constant methane emission rate). Each point in **Figure 4** represents the variability in the quantification at each individual target site. The total uncertainty of a quantification using MTDM is about 20%, and it includes method uncertainty and quantification variability of a source with a constant emission (Fredenslund et al., 2019). Emissions from the source are not constant over time when variability is higher than the total estimated uncertainty. Conversely, when variability is within the total uncertainty of a quantification, the former cannot be distinguished from the latter. The relatively high variability of the measured emissions in this study, as well as in other studies, clearly indicates that emissions from O&G infrastructure are not constant over time (e.g., Yacovitch et al., 2017; Zavala-Araiza et al., 2018; Tullos et al., 2021). At sources with constant emissions, variability has been observed to decrease in line with the number of plume traverses (Mønster et al., 2014). However, the investigated datasets did not show any correlation between variability on the quantification and the number of plume traverses: increasing the number of plume traverses did not decrease the variability of the quantified emission rates. At many of the investigated sites (especially at oil wells), it was clear that methane was emitted from the pump heads in pulses. This was evident from methane concentration measurements performed close to the wellheads.

Among the many ground-based remote-sensing methods applied to investigate O&G sites, only the MTDM is capable of revealing such important findings, because

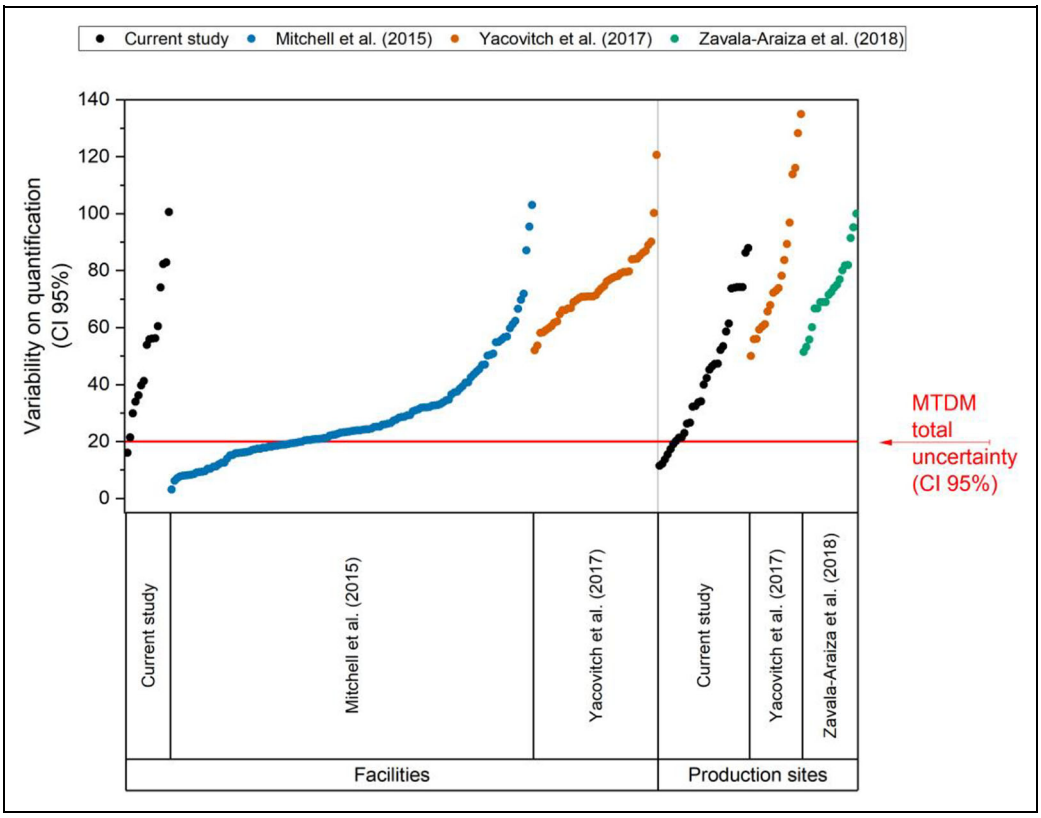

Figure 4. Quantification variability when using the mobile tracer gas dispersion method (MTDM)—a comparison with the literature. Maximum MTDM uncertainty is according to Fredenslund et al. (2019). Yacovitch et al. (2017) and Zavala-Araiza et al. (2018) report in their studies an asymmetric confidence interval due to the weighted mean emission rate. In the plot, the values reported by Yacovitch et al. (2017) and Zavala-Araiza et al. (2018) consider only the largest reported variability. CI stands for "confidence interval." DOI: https://doi.org/10.1525/elementa.2021.000111.f4

other methods have higher levels of uncertainty (e.g., GPM in Table S1) and/or lower temporal resolution (e.g., OTM 33A, U.S. EPA, 2014).

C_2H_6 emission rates and EFs

C_2H_6 emission rates ranged from $1.0{\cdot}10^{-4}$ to 78 kg h^{-1}, and they were positively skewed with a heavy tail (Table S10). Almost 80% of the sites, that is, 75 out of 95, exhibited a C_2H_6 emission rate below 1 kg h^{-1}, whereas only 3 sites had emission rates higher than 20 kg h^{-1}. A very small portion of the investigated sites (about 7%) contributed to about 77% of the total measured C_2H_6 emission rate (complete dataset in Figure S8A1) and had an emission rate higher than 9 kg h^{-1} (complete dataset in Figure S8A1). Very similar results can be obtained if the dataset is grouped into type of site (facilities and oil wells) and investigated region (Table S10 and Figure S8A). **Figure 5A** shows C_2H_6 emission rates from all 95 sites, grouped by the type of evaluation and type of site. The C_2H_6 EF with a 95% CI for the complete dataset was equal to 0.07 [0.04; 0.13] kg h^{-1} $site^{-1}$ (**Figure 5B2**). Among the investigated types of sites, facilities were the largest emitters with a C_2H_6 EF equal to 0.31 [0.08; 0.86] kg h^{-1} $site^{-1}$. Oil wells had a C_2H_6 EF equal to about 0.04 kg h^{-1} $site^{-1}$. Among the investigated regions, C6 reported the lowest C_2H_6 EF with a 95% CI equal to 0.03 [0.01; 0.07] kg h^{-1} $site^{-1}$, whereas regions C5A and C7 had C_2H_6 EFs equal to 0.16 and 0.19 kg h^{-1} $site^{-1}$, respectively. C_2H_6 EF values are reported in Table S12 and shown in **Figure 5B2**.

Comparison of C_2H_6 emissions reported in the literature comparison

Goetz et al. (2015) report C_2H_6 emission rates from 3 gas well pads located in the United States (Pennsylvania—Marcellus Shale), which are equal to 1.0, 5.0, and 17 kg h^{-1}, and therefore are within the emission rate interval reported by this study. The literature offers only 2 other studies from which to take a relatively large dataset of site-specific C_2H_6 emission rates (Yacovitch et al., 2015; Yacovitch et al., 2017). These studies explicitly report site-specific CH_4 emission rates and C_2H_6-to-CH_4 molar ratios, but they do not directly discuss C_2H_6 emission rates. Yacovitch et al. (2015) investigated 169 sites in Texas (Barnett Shale basin) by using the GPM, whereas Yacovitch et al. (2017) investigated 21 sites located in Colorado (DJ basin) and 49 sites in Arkansas (FV gas play) by using the MTDM. Both studies investigated a large variety of site types similar to the current study (including gathering facilities, production well pads, processing plants, and

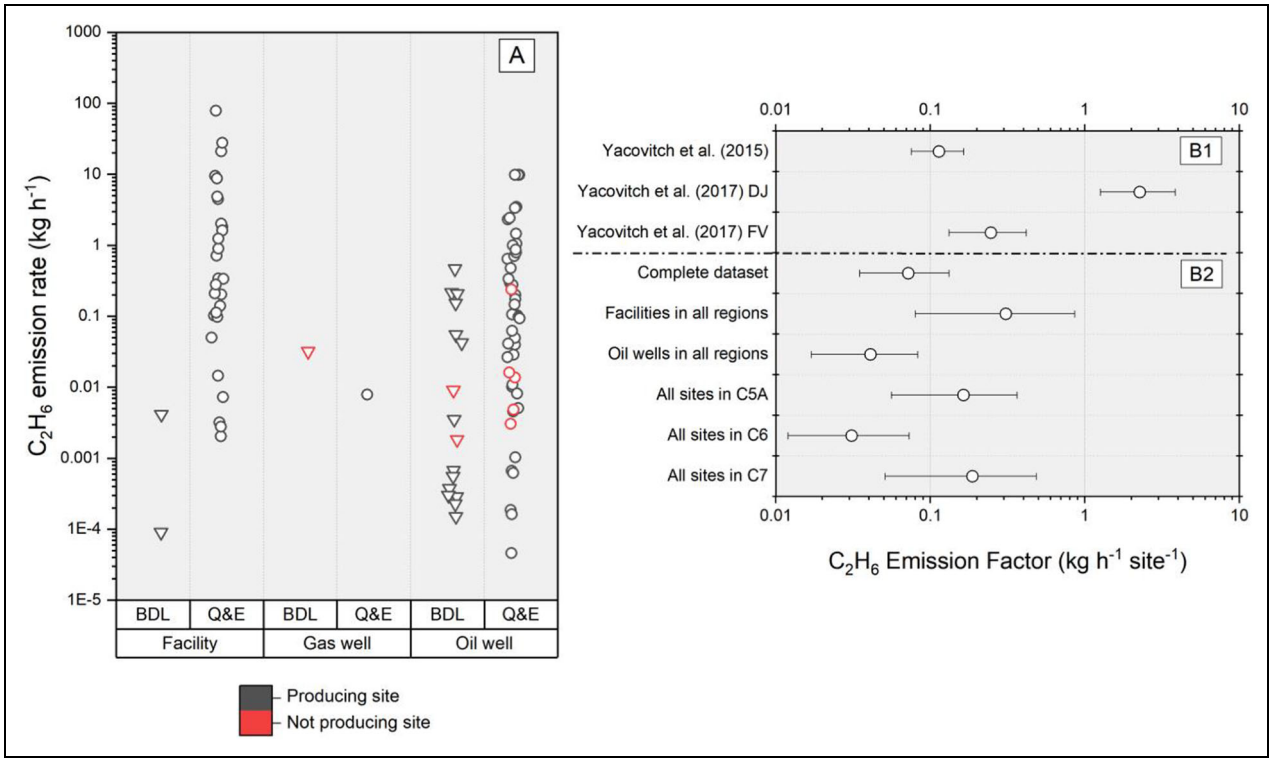

Figure 5. Overview of C_2H_6 emissions. (A) C_2H_6 emission rates grouped by type of site and type of evaluation: below detection limit (BDL), quantification and estimate (Q&E). (B1) C_2H_6 emission factors (EFs) of datasets available in the literature. (B2) C_2H_6 EF of datasets in the current study. Data for C_2H_6 EF are available in Table S11. DOI: https://doi.org/10.1525/elementa.2021.000111.f5

transmission pipes; Table S6). The complete dataset for the current study is the second largest available in the literature after Yacovitch et al. (2015), which counts 166 investigated sites. The available datasets are positively skewed with a heavy tail (Table S11 and Figure S8B). The complete dataset for the current study is the most skewed in the literature and includes the largest number of observations in the lowest range of emission rates (Figure S8B1 and Figure S8B2). EFs were calculated for all available literature datasets (**Figure 5** and Table S12). The complete dataset for the current study had the lowest C_2H_6 EF, whereas Yacovitch et al. (2017) DJ reported the highest C_2H_6 EF with a 95% CI equal to 2.27 [1.3; 3.9] kg h^{-1} $site^{-1}$.

C_2H_6-to-CH_4 molar ratio

The distribution of the measured C_2H_6-to-CH_4 molar ratios is shown in **Figure 6A**, while **Figure 6B** shows the results grouped by region and type of site. The location of the sites is shown in Figure S9. Most of the investigated sites were oil wells and facilities, while only one record referred to a gas well. None of the facilities had units with fuel combustion, and therefore the C_2H_6-to-CH_4 molar ratios were never affected by combustion—as also supported by observations when CO and CO_2 plume measurements were never detected. At facilities, the presence of separators and condensate storage tanks or controls on tanks (e.g., flare or vapor recovery) could have affected the C_2H_6-to-CH_4 molar ratios. In general, the C_2H_6-to-CH_4 molar ratio was small in region C5A, and large in regions C6 and C7. In the current study, detected values were between 0.3% and 91%, and thus in line with the literature, providing a C_2H_6-to-CH_4 molar ratio as small as 0.1% (Roscioli et al., 2015; Yacovitch et al., 2017) and as large as 100% (Yacovitch et al., 2015). Details about the isotopic signature of CH_4 emissions from Rumanian O&G sites are reported by Menoud et al. (2022).

Nonproducing wells

Among the 155 investigated wells, 20 were nonproducing wells (16 oil wells and 4 gas wells) representing 13% of the wells in the dataset (**Figures 2B**, **5A**, and **6B**). In the investigated area, defined as visited clusters, 16% of wells were nonproducing wells (432 out of 2,641). Therefore, the percentage of investigated nonproducing wells in the collected dataset was comparable to the true percentage of nonproducing wells in the investigated area. CH_4 emission rates from nonproducing wells ranged from 0.001 to 0.58 kg h^{-1}, and most of the investigated sites (65%) were BDL (**Figure 2B** and Table S13). Only 8 C_2H_6 emission rates were calculated at nonproducing wells, ranging from 0.002 to 0.24 kg h^{-1} (**Figure 5A** and Table S13). Due to the relatively high number of nonproducing wells in the investigated area, EFs were calculated to support the bottom-up analysis, even though the numbers of observations were limited. CH_4 EF with a 95% CI was equal to 0.04 [0.02; 0.08] kg h^{-1} $site^{-1}$, and C_2H_6 EF with a 95% CI was equal to 0.01 [0.004; 0.04] kg h^{-1} $site^{-1}$ (Table S14).

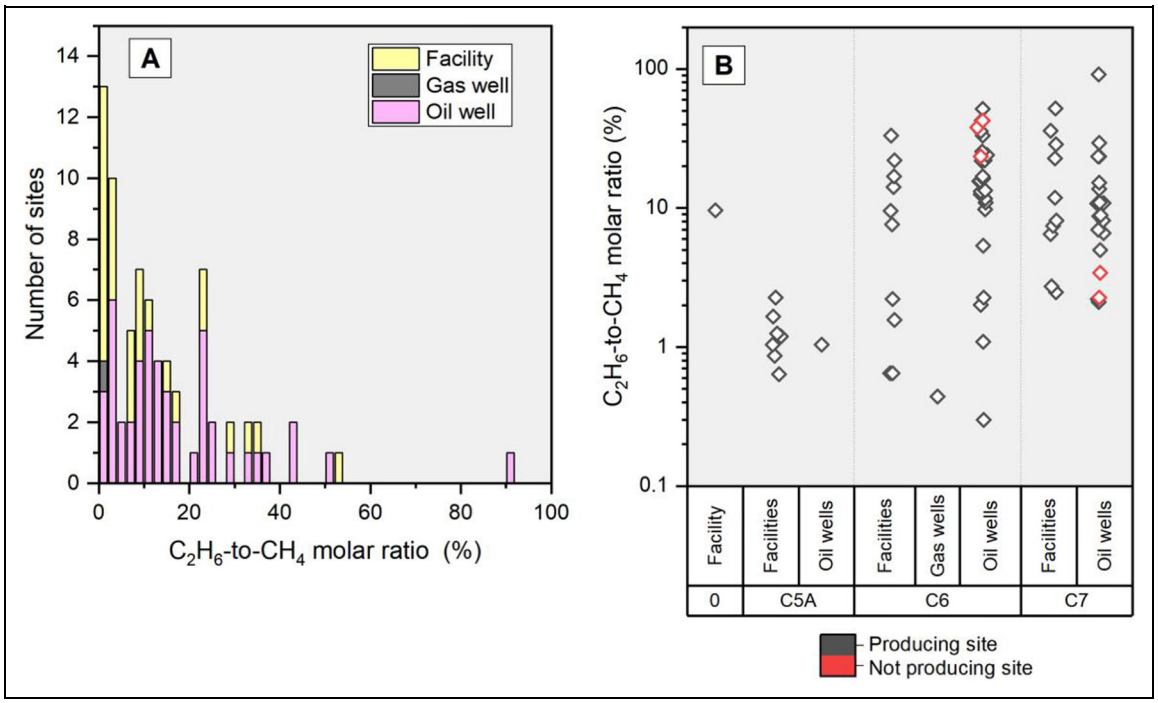

Figure 6. Overview of the C_2H_6-to-CH_4 molar ratio. (A) Distribution of the C_2H_6-to-CH_4 molar ratio at 76 sites. (B) C_2H_6-to-CH_4 molar ratio grouped by region and type of site. Location of regions 0, C5A, C6, and C7 can be found in **Figure 1**. DOI: https://doi.org/10.1525/elementa.2021.000111.f6

Conclusions

CH_4 emissions were investigated at 200 onshore O&G sites, which were mainly oil wells (61%), facilities (21%), and gas wells (17%). The main findings were as follows:

- CH_4 emission rates were highly skewed with a so-called "heavy tail," and they were represented by an EF with a 95% CI equal to 0.53 [0.32; 0.79] kg h^{-1} $site^{-1}$.
- Five percent of the sites contributed to about 52% of the total CH_4 emission rate. Targeting mitigation actions on these sites with high emission rates would be the most efficient.
- Twenty-eight percent of the investigated sites had CH_4 emissions BDL.
- In this study, the CH_4 EF fell within the range of the majority of the EFs (0.5 and 3.0 kg h^{-1} $site^{-1}$) reported in the literature for the O&G sector in North America.
- Calculating the CH_4 EF without observations BDL resulted in a higher value (2.3 [1.5; 3.5] kg h^{-1} $site^{-1}$), which could result in a misleading bottom-up analysis of CH_4 emissions in the investigated area.
- The only correlation that was found between CH_4 emission rates and production factors was in relation to oil wells, emissions from which were negatively correlated to produce wastewater. The lack of correlation with production factors excludes the possibility of using them for estimating CH_4 emissions in the O&G sector in the investigated area. Thus, direct measurements are the most reliable way to investigate CH_4 emissions.

C_2H_6 emissions were assessed at 95 of the 200 sites and were mainly investigated at oil wells (66%) and facilities (32%). The main findings as follows:

- As above, C_2H_6 emission rates were highly skewed with a so-called heavy tail, and they were represented by an EF with a 95% CI equal to 0.07 [0.04; 0.13] kg h^{-1} $site^{-1}$.
- Seven percent of the sites contributed to about 77% of the total C_2H_6 emission rate, with emission rates higher than 9 kg h^{-1}. As for CH_4 emissions, decreasing C_2H_6 emissions from just these few sites would significantly decrease the emission from the investigated area.
- C_2H_6 emissions rates quantified in Romania were more skewed in comparison to studies in the United States resulting in a lower C_2H_6 EF.

Data accessibility statement

The emission dataset associated with this submission is presented in Table S15 in the Supplementary Material.

Supplementary files

The supplemental files for this article can be found as follows:

Text S1. Supplementary Material, containing Sections S0–S9 (Word File).

Acknowledgment

The authors thank all the members of the ROMEO campaign, and in particular Konstantinos Kissas for his support in part of the measurements, and Thomas Röckman,

Stefan Schwietzke, and Daniel Zavala-Araiza for their feedback on the manuscript.

Funding

The Romanian Methane Emission from Oil & Gas (ROMEO) campaign was initiated as part of the MEMO^2 project, funded by the European Union's Horizon 2020 research and innovation programme under the Marie Skłodowska-Curie grant agreement No 722479. The ROMEO campaign was funded under the Climate and Clean Air Coalition (CCAC) Oil and Gas Methane Science Studies (MSS), hosted by the United Nations Environment Programme. Funding was provided by the Environmental Defense Fund, Oil and Gas Climate Initiative, European Commission and CCAC. Next to this funding, TNO received funding for measurements within the ROMEO campaign from DG ENER.

Competing interests

The authors have no competing interests to declare.

Author contributions

Contributed to conception and design: AD, CS, AH, IV.

Contributed to the acquisition of data: AD, CS, AH, IV, PB, ME.

Contributed to the analysis and interpretation of data: AD, CS, AH, IV, PB, ME.

Drafted and/or revised the article: AD, CS, AH, IV.

Approved the submitted version for publication: AD, CS, AH, IV, PB.

References

Aikin, AC, **Herman, JR**, **Maier, EJ**, **McQuillan, CJ**. 1982. Atmospheric chemistry of ethane and ethylene. *Journal of Geophysical Research* **87**: 3105–3118. DOI: http://dx.doi.org/10.1029/JC087iC04p03105.

Allen, D. 2016. Attributing atmospheric methane to anthropogenic emission sources. *Accounts of Chemical Research* **49**(7): 1344–1350. DOI: http://dx.doi.org/10.1021/acs.accounts.6b00081.

Allen, DT, Torres, VM, Thomas, J, Sullivan, DW, Harrison, M, Hendler, A, Herndon, SC, Kolb, CE, Fraser, MP, Hill, AD, Lamb, BK, Miskimins, J, Sawyer, RF, Seinfeld, JH. 2013. Measurements of methane emissions at natural gas production sites in the United States. *Proceedings of the National Academy of Sciences of the United States of America* **110**(44): 17768–17773. DOI: http://dx.doi.org/10.1073/pnas.1304880110.

Brandt, AR, **Heath, GA**, **Cooley, D**. 2016. Methane leaks from natural gas systems follow extreme distributions. *Environmental Science & Technology* **50**(22): 12512–12520. DOI: http://dx.doi.org/10.1021/acs.est.6b04303.

Brandt, AR, **Heath, GA**, **Kort, EA**, **O'Sullivan, F**, **Pétron, G**, **Jordaan, SM**, **Tans, P**, **Wilcox, J**, **Gopstein, AM**, **Arent, D**, **Wofsy, S**, **Brown, NJ**, **Bradley, R**, **Stucky, GD**, **Eardley, D**, **Harriss, R**. 2014. Methane leaks from North American natural gas systems. *Science* **343**(6172): 733–735. DOI: http://dx.doi.org/10.1126/science.1247045.

Brantley Halley, L, **Thoma, ED**, **Squier, WC**, **Guven, BB**, **Lyon, D**. 2014. Assessment of methane emissions from oil and gas production pads using mobile measurements. *Environmental Science & Technology* **48**(24): 14508–14515. DOI: http://dx.doi.org/10.1021/es503070q.

Briggs, GA. 1974. *Diffusion estimation for small emissions*. Oak Ridge, TN. DOI: http://dx.doi.org/10.2172/5118833.

Caulton, DR, **Li, Q**, **Bou-Zeid, E**, **Fitts, JP**, **Golston, LM**, **Pan, D**, **Lu, J**, **Lane, HM**, **Buchholz, B**, **Guo, X**, **McSpiritt, J**, **Wendt, L**, **Zondlo, MA**. 2018. Quantifying uncertainties from mobile-laboratory-derived emissions of well pads using inverse Gaussian methods. *Atmospheric Chemistry and Physics* **18**(20): 15145–15168. DOI: http://dx.doi.org/10.5194/acp-18-15145-2018.

Chernick, MR, **LaBudde, RA**. 2011. *An introduction to bootstrap methods with applications to R*. Hoboken, NJ: John Wiley & Sons.

Climate and Clean Air Coalition. 2021. Oil & gas. Measuring & minimizing mineral methane emissions and reducing black carbon through flaring (Mineral Methane Initiative). Available at https://www.ccacoalition.org/en/initiatives/oil-gas. Accessed 23 May 2022.

Collins, WJ, **Derwent, RG**, **Johnson, CE**, **Stevenson, DS**. 2002. Troposphere and their global warming potentials. *Climate Change* **52**(2): 453–479. Available at http://www.springerlink.com/index/141XDT79CVKDC7UH.pdf.

Delre, A. 2018. *Greenhouse gas emissions from wastewater treatment plants: Measurements and carbon footprint assessment*. Technical University of Denmark. Available at https://orbit.dtu.dk/en/publications/greenhouse-gas-emissions-from-wastewater-treatment-plants-measure.

Delre, A, **Mønster, J**, **Samuelsson, J**, **Fredenslund, AM**, **Scheutz, C**. 2018. Emission quantification using the tracer gas dispersion method: The influence of instrument, tracer gas species and source simulation. *Science of the Total Environment* **634**: 59–66. DOI: http://dx.doi.org/10.1016/j.scitotenv.2018.03.289.

Delre, A, **Mønster, J**, **Scheutz, C**. 2017. Greenhouse gas emission quantification from wastewater treatment plants, using a tracer gas dispersion method. *Science of the Total Environment* **605–606**: 258–268. DOI: http://dx.doi.org/10.1016/j.scitotenv.2017.06.177.

Dinu, C, **Morariu, DC**, **Mocanu, VI**. 1996. Hydrocarbon resources of Romania—A review, in Wessely, G, Liebl, W eds., *Oil and gas in Alipidic thrustbelts and basins of central and eastern Europe*. Vienna, Austria: European Association Geoscientists and Engineers Special Publication; Vol. 5: 23–28.

European Commission. 2019. The European Green Deal of the European Commission. COM/2019/640. Available at https://eur-lex.europa.eu/legal-content/EN/TXT/?uri=COM%3A2019%3A640%3AFIN. Accessed 13 March 2022.

European Commission. 2020. EU strategy to reduce methane emissions. COM/2020/663. Available at https://eur-lex.europa.eu/legal-content/EN/TXT/?uri=CELEX%3A52020DC0663&qid=1647116210947. Accessed 13 March 2022.

Fredenslund, AM, **Mønster, J**, **Kjeldsen, P**, **Scheutz, C**. 2019. Development and implementation of a screening method to categorise the greenhouse gas mitigation potential of 91 landfills. *Waste Management* **87**: 915–923. DOI: http://dx.doi.org/10.1016/j.wasman.2018.03.005.

Fredenslund, AM, **Rees-White, TC**, **Beaven, RP**, **Delre, A**, **Finlayson, A**, **Helmore, J**, **Allen, G**, **Scheutz, C**. 2019. Validation and error assessment of the mobile tracer gas dispersion method for measurement of fugitive emissions from area sources. *Waste Management* **83**: 68–78. DOI: http://dx.doi.org/10.1016/j.wasman.2018.10.036.

Goetz, JD, **Floerchinger, C**, **Fortner, EC**, **Wormhoudt, J**, **Massoli, P**, **Knighton, WB**, **Herndon, SC**, **Kolb, CE**, **Knipping, E**, **Shaw, SL**, **DeCarlo, PF**. 2015. Atmospheric emission characterization of Marcellus shale natural gas development sites. *Environmental Science & Technology* **49**(11): 7012–7020. DOI: http://dx.doi.org/10.1021/acs.est.5b00452.

Harriss, R, **Alvarez, RA**, **Lyon, D**, **Zavala-Araiza, D**, **Nelson, D**, **Hamburg, SP**. 2015. Using multi-scale measurements to improve methane emission estimates from oil and gas operations in the Barnett Shale region, Texas. *Environmental Science & Technology* **49**(13): 7524–7526. DOI: http://dx.doi.org/10.1021/acs.est.5b02305.

Hensen, A, **Groot, TT**, **Van Den Bulk, WCM**, **Vermeulen, AT**, **Olesen, JE**, **Schelde, K**. 2006. Dairy farm CH4 and N2O emissions, from one square metre to the full farm scale. *Environmental Science & Technology* **112**(2–3): 146–152. DOI: http://dx.doi.org/10.1016/j.agee.2005.08.014.

Hensen, A, **Scharff, H**. 2001. Methane emission estimates from landfills obtained with dynamic plume measurements. *Water, Air, & Soil Pollution: Focus* **1**: 455–464. DOI: http://dx.doi.org/10.1007/978-94-010-9026-1_45.

Highwood, EJ, **Shine, KP**, **Hurley, MD**, **Wallington, TJ**. 1999. Estimation of direct radiative forcing due to non-methane hydrocarbons. *Atmospheric Environment* **33**(5): 759–767. DOI: http://dx.doi.org/10.1016/S1352-2310(98)00220-9.

International Energy Agency. 2020. Methane Tracker 2020 of the International Energy Agency. Paris, France. Available at https://www.iea.org/reports/methane-tracker-2020. Accessed 19 October 2020.

Johnson, MR, **Tyner, DR**, **Conley, S**, **Schwietzke, S**, **Zavala-Araiza, D**. 2017. Comparisons of airborne measurements and inventory estimates of methane emissions in the Alberta upstream Oil and Gas sector. *Environmental Science & Technology* **51**(21): 13008–13017. DOI: http://dx.doi.org/10.1021/acs.est.7b03525.

Kirschke, S, **Bousquet, P**, **Ciais, P**, **Saunois, M**, **Canadell, JG**, **Dlugokencky, EJ**, **Bergamaschi, P**, **Bergmann, D**, **Blake, DR**, **Bruhwiler, L**, **Cameron-Smith, P**, **Castaldi, S**, **Chevallier, F**, **Feng, L**, **Fraser, A**, **Heimann, M**, **Hodson, EL**, **Houweling, S**, **Josse, B**, **Fraser, PJ**, **Krummel, PB**, **Lamarque, J-F**, **Langenfelds, RL**, **Le Quéré, C**, **Naik, V**, **O'Doherty, S**, **Palmer, PI**, **Pison, I**, **Plummer, D**, **Poulter, B**, **Prinn, RG**, **Rigby, M**, **Ringeval, B**, **Santini, M**, **Schmidt, M**, **Shindell, DT**, **Simpson, IJ**, **Spahni, R**, **Steele, LP**, **Strode, SA**, **Sudo, K**, **Szopa, S**, **van der Werf, GR**, **Voulgarakis, A**, **van Weele, M**, **Weiss, RF**, **Williams, JE**, **Zeng, G**. 2013. Three decades of global methane sources and sinks. *Nature Geoscience* **6**(10): 813–823. DOI: http://dx.doi.org/10.1038/ngeo1955.

Lamb, BK, **Mcmanus, JB**, **Shorter, JH**, **Kolb, CE**, **Mosher, B**, **Harriss, RC**, **Allwine, E**, **Blaha, D**, **Howard, T**, **Guenther, A**, **Lott, RA**, **Siverson, R**, **Westburg, H**, **Zimmerman, P**. 1995. Development of atmospheric tracer methods to measure methane emissions from natural gas facilities and urban areas. *Environmental Science & Technology* **29**(6): 1468–1479. DOI: http://dx.doi.org/10.1021/es00006a007.

Lan, X, **Talbot, R**, **Laine, P**, **Torres, A**. 2015. Characterizing fugitive methane emissions in the Barnett Shale area using a mobile laboratory. *Environmental Science & Technology* **49**(13): 8139–8146. DOI: http://dx.doi.org/10.1021/es5063055.

Menoud, M, **van der Veen, C**, **Maazallahi, H**, **Hensen, A**, **Velzeboer, I**, **van den Bulk, P**, **Delre, A**, **Korben, P**, **Schwietzke, S**, **Ardelean, M**, **Calcan, A**, **Etiope, G**, **Baciu, C**, **Scheutz, C**, **Schmidt, M**, **Röckmann, T**. 2022. CH_4 isotopic signatures of emissions from oil and gas extraction sites in Romania. *Elementa: Science of the Anthropocene* **10**(1). DOI: https://doi.org/10.1525/elementa.2021.000092.

Mielke-Maday, I, **Schwietzke, S**, **Yacovitch, TI**, **Miller, B**, **Conley, S**, **Kofler, J**, **Handley, P**, **Thorley, E**, **Herndon, SC**, **Hall, B**, **Dlugokencky, E**, **Lang, P**, **Wolter, S**, **Moglia, E**, **Crotwell, M**, **Crotwell, A**, **Rhodes, M**, **Kitzis, D**, **Vaughn, T**, **Bell, C**, **Zimmerle, D**, **Schnell, R**, **Pétron, G**. 2019. Methane source attribution in a U.S. dry gas basin using spatial patterns of ground and airborne ethane and methane measurements. *Elementa: Science of the Anthropocene* **7**(13). DOI: http://dx.doi.org/10.1525/elementa.351.

Mika, B, **Daniel, Y**. 2021. *R package named "tidyboot": Tidyverse-Compatible Bootstrapping*. Available at https://cran.r-project.org/web/packages/tidyboot/index.html. Accessed 23 May 2022.

Millard, SP. 2013. *EnvStats: An R package for environmental statistics*. 2nd edition. New York, NY: Springer. DOI: http://dx.doi.org/10.1007/978-1-4614-8456-1.

Mitchell, AL, **Tkacik, DS**, **Roscioli, JR**, **Herndon, SC**, **Yacovitch, TI**, **Martinez, DM**, **Vaughn, TL**, **Williams, LL**, **Sullivan, MR**, **Floerchinger, C**, **Omara, M**, **Subramanian, R**, **Zimmerle, D**, **Marchese, AJ**, **Robinson, AL.** 2015. Measurements of methane

emissions from natural gas gathering facilities and processing plants: Measurement results. *Environmental Science & Technology* **49**(5): 3219−3227. DOI: http://dx.doi.org/10.1021/es5052809.

Mønster, J, **Samuelsson, J**, **Kjeldsen, P**, **Rella, CW**, **Scheutz, C**. 2014. Quantifying methane emission from fugitive sources by combining tracer release and downwind measurements: A sensitivity analysis based on multiple field surveys. *Waste Management* **34**: 1416–1428. DOI: http://dx.doi.org/10.1016/j.wasman.2014.03.025.

O'Connell, E, **Risk, D**, **Atherton, E**, **Bourlon, E**, **Fougère, C**, **Baillie, J**, **Lowry, D**, **Johnson, J**. 2019. Methane emissions from contrasting production regions within Alberta, Canada: Implications under incoming federal methane regulations. *Elementa: Science of the Anthropocene* **7**(3). DOI: http://dx.doi.org/10.1525/elementa.341.

Omara, M, **Sullivan, MR**, **Li, X**, **Subramian, R**, **Robinson, AL**, **Presto, AA**. 2016. Methane emissions from conventional and unconventional natural gas production sites in the Marcellus Shale basin. *Environmental Science & Technology* **50**(4): 2099–2107. DOI: http://dx.doi.org/10.1021/acs.est.5b05503.

OriginLab. 2019. Origin Pro. Available at https://www.originlab.com/. Accessed 19 October 2020.

Pasquill, F. 1974. *Atmospheric diffusion*. Halsted Press, edition; 2nd edition. New York, NY: Wiley.

Pawlewicz, M. 2007. Total petroleum systems of the Carpathian–Balkanian Basin Province of Romania and Bulgaria: U.S. Geological Survey Bulletin 2204–F. Available at http://pubs.usgs.gov/bul/2204/f/. Accessed 23 May 2022.

Peischl, **J**, **Eilerman, SJ**, **Neuman, JA**, **Aikin, KC**, **de Gouw**, **J**, **Gilman, JB**, **Herndon, SC**, **Nadkarni, R**, **Trainer, M**, **Warneke, C**, **Ryerson, TB**. 2018. Quantifying methane and ethane emissions to the atmosphere from central and Western U.S. oil and natural gas production regions. *Journal of Geophysical Research: Atmospheres* **123**(14): 7725–7740. DOI: http://dx.doi.org/10.1029/2018JD028622.

Prather, MJ, **Holmes, CD**, **Hsu, J**. 2012. Reactive greenhouse gas scenarios: Systematic exploration of uncertainties and the role of atmospheric chemistry. *Geophysical Research Letters* **39**(9): 6–10. DOI: http://dx.doi.org/10.1029/2012GL051440.

Reimann, C, **Filzmoser, P**, **Garrett, RG**, **Dutter, R**. 2008. *Statistical data analysis explained: Applied environmental statistics with R*. Chichester, UK: John Wiley & Sons, Ltd. DOI: http://dx.doi.org/10.1002/9780470987605.

Rella, CW, **Tsai, TR**, **Botkin, CG**, **Crosson, ER**, **Steele, D**. 2015. Measuring emissions from oil and natural gas well pads using the mobile flux plane technique. *Environmental Science & Technology* **49**(7): 4742–4748. DOI: http://dx.doi.org/10.1021/acs.est.5b00099.

Riddick, SN, **Mauzerall, DL**, **Celia, MA**, **Kang, M**, **Bressler, K**, **Chu, C**, **Gum, CD**. 2019. Measuring methane emissions from abandoned and active oil and gas wells in West Virginia. *Science of the Total Environment* **651**: 1849–1856. DOI: http://dx.doi.org/10.1016/j.scitotenv.2018.10.082.

Robertson, AM, **Edie, R**, **Snare, D**, **Soltis, J**, **Field, RA**, **Burkhart, MD**, **Bell, CS**, **Zimmerle, D**, **Murphy, SM**. 2017. Variation in methane emission rates from well pads in four oil and gas basins with contrasting production volumes and compositions. *Environmental Science & Technology* **51**(15): 8832–8840. DOI: http://dx.doi.org/10.1021/acs.est.7b00571.

Röckmann, T, **the ROMEO Team**. 2020. ROMEO - ROmanian Methane Emissions from Oil & gas. EGU General Assembly 2020, Online, 4–8 May 2020: EGU2020-18801. DOI: http://dx.doi.org/10.5194/egusphere-egu2020-18801.

Roscioli, JR, Herndon, SC, Yacovitch, TI, Knighton, WB, Zavala-Araiza, D, Johnson, MR, Tyner, DR. 2018. Characterization of methane emissions from five cold heavy oil production with sands (CHOPS) facilities. *Journal of the Air & Waste Management Association* **68**(7): 671–684. DOI: http://dx.doi.org/10.1080/10962247.2018.1436096.

Roscioli, JR, **Yacovitch, TI**, **Floerchinger**, **C**, **Mitchell, AL**, **Tkacik, DS**, **Subramanian**, **R**, **Martinez, DM**, **Vaughn, TL**, **Williams, L**, **Zimmerle, D**, **Robinson, AL**, **Herndon, SC**, **Marchese, AJ**. 2015. Measurements of methane emissions from natural gas gathering facilities and processing plants: measurement methods. *Atmospheric Measurement Techniques* **8**(5): 2017–2035. DOI: http://dx.doi.org/10.5194/amt-8-2017-2015.

Samuelsson, J, **Delre, A**, **Tumlin, S**, **Hadi, S**, **Offerle, B**, **Scheutz, C**. 2018. Optical technologies applied alongside on-site and remote approaches for climate gas emission quantification at a wastewater treatment plant. *Water Research* **131**: 299–309. Elsevier Ltd. DOI: http://dx.doi.org/10.1016/j.watres.2017.12.018.

Scheutz, C, **Samuelsson, J**, **Fredenslund, AM**, **Kjeldsen, P**. 2011. Quantification of multiple methane emission sources at landfills using a double tracer technique. *Waste Management* **31**: 1009–1017. Elsevier Ltd. DOI: http://dx.doi.org/10.1016/j.wasman.2011.01.015.

Schwietzke, S, **Griffin, WM**, **Matthews, HS**, **Bruhwiler, LMP**. 2014a. Natural gas fugitive emissions rates constrained by global atmospheric methane and ethane. *Environmental Science Technology* **48**(14): 7714–7722. DOI: http://dx.doi.org/10.1021/es501204c.

Schwietzke, S, **Griffin, WM**, **Matthews, HS**, **Bruhwiler, LMP**. 2014b. Global bottom-up fossil fuel fugitive methane and ethane emissions inventory for atmospheric modeling. *ACS Sustainable Chemistry & Engineering* **2**(8): 1992–2001. DOI: http://dx.doi.org/10.1021/sc500163h.

Shindell, D, **Kuylenstierna, JCI**, **Vignati, E**, **Van Dingenen, R**, **Amann, M**, **Klimont, Z**, **Anenberg, SC**, **Muller, N**, **Janssens-Maenhout, G**, **Raes, F**, **Schwartz, J**, **Faluvegi, G**, **Pozzoli, L**, **Kupiainen,**

K, **Höglund-Isaksson, L**, **Emberson, L**, **Streets, D**, **Ramanathan, V**, **Hicks, K**, **Kim Oanh, NT**, **Milly, G**, **Williams, M**, **Demkine, V**, **Fowler, D**. 2012. Simultaneously mitigating near-term climate change and improving human health and food security. *Science* **335**(6065): 183–189. DOI: http://dx.doi.org/10.1126/science.1210026.

Shorter, JH, **McManus, JB**, **Kolb, CE**, **Allwine, EJ**, **Siverson, R**, **Lamb, BK**, **Mosher, BW**, **Harriss, RC**, **Howard, T**, **Lott, RA**. 1997. Collection of leakage statistics in the natural gas system by tracer methods. *Environmental Science & Technology* **31**(7): 2012–2019. DOI: http://dx.doi.org/10.1021/es9608095.

Shrivastava, A, **Gupta, V**. 2011. Methods for the determination of limit of detection and limit of quantitation of the analytical methods. *Chronicles of Young Scientists* **2**(1): 21–25. DOI: http://dx.doi.org/10.4103/2229-5186.79345.

Simpson, IJ, Andersen, MPS, Meinardi, S, Bruhwiler, L, Blake, NJ, Helmig, D, Sherwood Rowland, F, Blake, DR. 2012. Long-term decline of global atmospheric ethane concentrations and implications for methane. *Nature* **488**(7412): 490–494. DOI: http://dx.doi.org/10.1038/nature11342.

Smith, ML, **Kort, EA**, **Karion, A**, **Sweeney, C**, **Herndon, SC**, **Yacovitch, TI**. 2015. Airborne ethane observations in the Barnett Shale: Quantification of ethane flux and attribution of methane emissions. *Environmental Science & Technology* **49**(13): 8158–8166. DOI: http://dx.doi.org/10.1021/acs.est.5b00219.

Stocker, TF, **Qin, D**, **Plattner, G-K**, **Tignor, M**, **Allen, SK**, **Boschung, J**, **Nauels, A**, **Xia, Y**, **Bex, V**, **Midgley, PM eds.** 2013. *IPCC, 2013: Climate change 2013: The physical science basis*. Contribution of Working Group I to the Fifth Assessment Report of the Intergovernmental Panel on Climate Change. Cambridge, UK. Available at http://www.ipcc.ch/pdf/assessment-report/ar5/wg1/WG1AR5_Frontmatter_FINAL.pdf.

Tari, G, **Dicea, O**, **Larfargue, E**, **Ellouz, N**, **Roure, F**, **Georgiev, G**, **Popov, S**, **Mihai, S**, **Weir, G**. 1997. Cimmerian and alpine stratigraphy and structural evolution of the Moesian platform (Romania/Bulgaria), in *Regional and petroleum geology of the Black Sea surrounding region* (**Vol. 68**). Tulsa, OK: American Association of Petroleum Geologists Memoir: 63–90.

Tullos, EE, **Stokes, SN**, **Cardoso-Saldaña, FJ**, **Herndon, SC**, **Smith, BJ**, **Allen, DT**. 2021. Use of short duration measurements to estimate methane emissions at oil and gas production sites. *Environmental Science & Technology Letters* **8**(6): 463–467. DOI: http://dx.doi.org/10.1021/acs.estlett.1c00239.

United Nations Framework Convention on Climate Change. 2020. *National inventory submissions*. Available at https://unfccc.int/ghg-inventories-annex-i-parties/2020. Accessed 19 October 2020.

U.S. EPA. 2014. *Other Test Method 33A: Geospatial Measurement of Air Pollution, Remote Emissions Quantification—Direct Assessment (GMAP-REQ-DA)*. Air Emission Measurement Center of US EPA. Available at https://www.epa.gov/sites/production/files/2020-08/documents/otm33a.pdf. Accessed 19 October 2020.

U.S. EPA. 2018. EPA handbook: Optical and remote sensing for measurement and monitoring of emissions flux of gases and particulate matter. Available at https://www.epa.gov/sites/default/files/2018-08/documents/gd-52v.2.pdf. Accessed 23 May 2022.

Yacovitch, TI, **Daube, C**, **Vaughn, TL**, **Bell, CS**, **Roscioli, JR**, **Knighton, WB**, **Nelson, DD**, **Zimmerle, D**, **Pétron, G**, **Herndon, SC**. 2017. Natural gas facility methane emissions: Measurements by tracer flux ratio in two US natural gas producing basins. *Elementa: Science of the Anthropocene* **5**(69). DOI: http://dx.doi.org/10.1525/elementa.251.

Yacovitch, TI, **Herndon, SC**, **Pétron, G**, **Kofler, J**, **Lyon, D**, **Zahniser, MS**, **Kolb, CE**. 2015. Mobile laboratory observations of methane emissions in the Barnett Shale region. *Environmental Science & Technology* **49**(13): 7889–7895. DOI: http://dx.doi.org/10.1021/es506352j.

Yacovitch, TI, **Neininger, B**, **Herndon, SC**, **Van Der Gon, HD**, **Jonkers, S**, **Hulskotte, J**, **Roscioli, JR**, **Zavala-Araiza, D**. 2018. Methane emissions in the Netherlands: The Groningen field. *Elementa: Science of the Anthropocene* **6**. DOI: http://dx.doi.org/10.1525/elementa.308.

Zavala-Araiza, D, **Herndon, SC**, **Roscioli, JR**, **Yacovitch, TI**, **Johnson, MR**, **Tyner, DR**, **Omara, M**, **Knighton, B**. 2018. Methane emissions from oil and gas production sites in Alberta, Canada. *Elementa: Science of the Anthropocene* **6**(27). DOI: http://dx.doi.org/10.1525/elementa.284.

How to cite this article: Delre, A, Hensen, A, Velzeboer, I, van den Bulk, P, Edjabou, ME, Scheutz, C. 2022. Methane and ethane emission quantifications from onshore oil and gas sites in Romania, using a tracer gas dispersion method. *Elementa: Science of the Anthropocene* 10(1). DOI: https://doi.org/10.1525/elementa.2021.000111

Domain Editor-in-Chief: Detlev Helmig, Boulder AIR LLC, Boulder, CO, USA

Guest Editor: David Lowry, Royal Holloway University of London, Egham Hill, Egham, UK

Knowledge Domain: Atmospheric Science

Part of an Elementa Forum: Oil and Natural Gas Development: Air Quality, Climate Science, and Policy

Published: June 8, 2022 **Accepted:** April 26, 2022 **Submitted:** November 25, 2021

ELEMENTA Science of the Anthropocene

Elem Sci Anth is a peer-reviewed open access journal published by University of California Press.

OPEN ACCESS